

Analysis of Multicomponent Diffusion in Pore Networks

Diffusion flux models are developed for isobaric diffusion of a multicomponent gas mixture in pore networks of distributed pore size and length constructed by arranging pore segments around the bonds of a lattice of constant coordination number. Eigenvalue-eigenvector analysis is used to decompose the dusty-gas model equations, written for each pore segment in the network, into a set of independent single-species diffusion problems, each of which is then treated by combining the effective medium theory for resistor networks with the smooth field approximation (Burganos and Sotirchos, 1987). Results for a ternary mixture diffusing in a porous slab show that direct application of the smooth field approximation underestimates significantly the mass transport resistance.

**Stratis V. Sotirchos,
Vasilis N. Burganos**

Department of Chemical Engineering
University of Rochester
Rochester, NY 14627

Introduction

Because of its importance in the study of catalytic and non-catalytic gas-solid reactions occurring in porous media, the problem of multicomponent gaseous diffusion in porous structures has attracted much attention in the literature; as a result, numerous articles, reviews, and monographs dealing with it have appeared (Jackson, 1977; Cunningham and Williams, 1980; Mason and Malinauskas, 1983). Before diffusion flux models for porous media are developed, a physical model must be constructed for the porous structure, which is used as a basis for the analysis of multicomponent diffusion problem and, hence, for the development of appropriate flux expressions. Review of the relevant literature shows that structural models that consider porous structures consisting of an assemblage of straight cylindrical pores are among the most frequently used structural models, basically a consequence of the fact that the mass transport problem in single cylindrical capillaries has been extensively investigated.

The development of diffusion flux models for pore networks usually involves use of an appropriate flux model to describe the coupling of diffusion fluxes and concentration gradients in each cylindrical pore segment, followed by averaging of the diffusion fluxes for a single pore segment over all pore sizes and pore orientations. It must be pointed out that such an approach tacitly accepts the existence of long cylindrical pore segments between successive pore intersections, an assumption that may

break down at relatively high porosities. The dusty-gas model (Deriagin and Bakanov, 1957; Mason et al., 1967) is most frequently used to describe the multicomponent diffusion process in the transition regime, i.e., between the two limiting cases of Knudsen and molecular diffusion, in a single cylindrical capillary. The dusty-gas model flux expressions for isobaric diffusion may be obtained by considering that the total pressure drop of each species in the mixture is due to the additive effect of two momentum transfer processes, the rate of momentum transfer to the wall and the rate of momentum transfer arising from collisions of unlike molecules (Scott and Dullien, 1962; Silveston, 1964). In the formal development of the dusty-gas model (Mason and Malinauskas, 1983), however, the attendant flux expressions are obtained by viewing the porous structure as a collection of solid spheres held, with the aid of some external force, stationary in space and obstructing the motion of the gas molecules. The resulting flux expressions involve adjustable effective binary and Knudsen diffusion coefficients, which for a cylindrical capillary become the binary molecular diffusivities and the Knudsen diffusivities in the capillary.

The averaging of the diffusion fluxes for a single pore over all pore sizes and pore orientations is greatly facilitated by assuming a "thoroughly interconnected" pore network, which in more concrete terms translates into assuming that the microscopic concentration field in the pore network coincides with the macroscopic concentration field imposed over the porous medium, i.e., what Jackson (1977) calls the smooth field approximation. The smooth field approximation is mathematically expressed by setting the concentration gradient in a pore equal to the pro-

Correspondence concerning this paper should be addressed to S.V. Sotirchos.

jection of the macroscopic concentration gradient on the pore axis. Such an approach was employed by Feng and Stewart (1973), who developed a general class of flux models for multi-component diffusion in pore networks by extending earlier work by Johnson and Stewart (1965) for binary diffusion.

The flux expressions obtained by the above procedure reduce to the dusty-gas model form only for pore networks consisting of pores of the same size (homoporous solids). For heteroporous networks, the form of the obtained flux expressions is computationally involved since it entails matrix inversion of the dusty-gas model equations and subsequent averaging of the elements of the inverse matrix over the pore size and orientation distributions. In their collocation analysis of multicomponent diffusion in porous solids, Sørensen and Stewart (1982) employed low-order (first or second) quadratures to compute the average elements of the inverse matrix. Other investigators chose to directly apply the dusty-gas model equations to heteroporous solids by using effective binary and Knudsen diffusion coefficients given by empirical correlations or obtained through averaging of the binary diffusion coefficients of the Knudsen diffusivities in single pores over the pore size distribution (Chen and Rinker, 1979; Sotirchos and Amundson, 1984; Bliet et al., 1986). Further simplifications of the multicomponent flux expressions, such as consideration of pseudobinary mixtures and assumption of negligible cross-diffusion terms in the dusty-gas model (Černá et al., 1978), have also been presented, but such approaches are far from being reliable in general.

The validity of the smooth field approximation, as well as of the related flux models, is strictly restricted to special types of pore networks since it, in general, violates the mass balance equations at the nodes of the network. To overcome this problem, a different approach was taken by Burganos and Sotirchos (1987) for the analysis of trace diffusion in pore networks of constant coordination number. This approach makes use of the effective medium theory for resistor networks developed by Kirkpatrick (1973). The effective medium theory (EMT) is used to replace the original network by a network of pores of uniform (diffusional) conductance that is further analyzed by using the smooth field approximation (EMT-SFA procedure). Numerical computations for a variety of pore networks and pore size distributions confirmed the accuracy of the EMT-SFA method for effective diffusivity estimations. It was also shown that direct application of the smooth field approximation to the original network produces unacceptable overestimations of the effective diffusivity, which can even be as large as some orders of magnitude.

This paper presents the application of the above procedure, which has so far been established for self- or trace diffusion only (Burganos and Sotirchos, 1987), to the problem of multicomponent, isobaric diffusion of gases in pore networks. The extension is accomplished by introducing a sequence of matrix manipulations based on eigenvalue-eigenvector analysis which is used to decompose the dusty-gas model equations, as applied to a single pore, into a set of n (for n species) independent flux expressions (of the Fick's law type) for n auxiliary species whose concentration gradients and fluxes are pore size independent, linear combinations of the concentration gradients and fluxes of the actual species in the pore. Each independent diffusion problem can then be treated by the EMT-SFA procedure, by direct application of the smooth field approximation, or by any other averaging procedure applicable. The structure of the resulting

flux expressions is used to obtain indications as to why the dusty-gas model equations appear to be successful in correlating experimental data even for heteroporous solids.

Diffusion of Binary Mixtures in Pore Networks

We first extend the EMT-SFA procedure, which has so far been established for self- or trace diffusion only, to the analysis of the problem of binary diffusion in pore networks. This extension is basically straightforward, but it gives us an opportunity to briefly introduce the main points of the EMT-SFA before undertaking the analysis of the more complex problem of multicomponent diffusion.

As in our previous work (Burganos and Sotirchos, 1987), we consider pore networks consisting of long, straight, cylindrical capillaries of nonuniform radius and length arranged around the bonds of two- or three-dimensional lattices of uniform coordination number. Two-dimensional pore networks are understood as being embedded in a slice of the porous medium. A two-dimensional network of pores of nonuniform radius and length with coordination number equal to 4 is shown in Figure 1. For a diffusing mixture of A and B in a pore segment k , we can write in the absence of chemical reaction for the steady state flux of A , under isobaric conditions,

$$\underline{N}_{Ak} = -D_{Ak} \nabla c_{Ak} \quad (1)$$

where D_{Ak} is the diffusion coefficient of A in pore k and ∇c_{Ak} is the concentration gradient along the pore. The diffusion coefficient of A is given by the expression

$$D_{Ak} = \frac{1}{\frac{1}{D_{KA,k}} + \frac{1 - \gamma x_{Ak}}{D_{AB}}} \quad (2)$$

In Eq. 2, $D_{KA,k}$ is the Knudsen diffusivity of A in pore k , D_{AB} is the binary molecular diffusivity of the (A, B) pair, x_{Ak} is the mole fraction of A in the same pore segment, and γ is given by

$$\gamma = 1 - \sqrt{\frac{M_A}{M_B}}$$

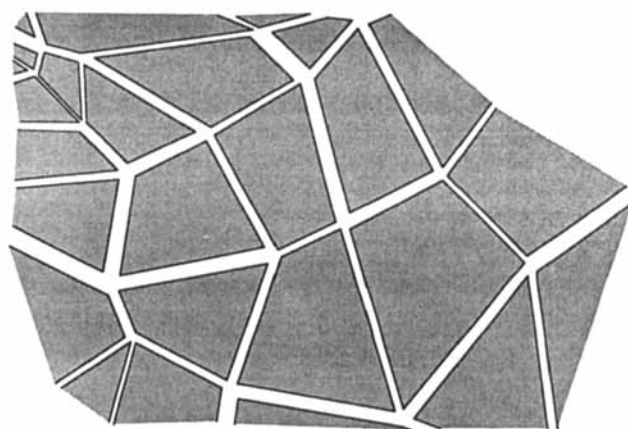


Figure 1. Sample of a two-dimensional pore network with $z = 4$ and nonuniform pore radius and length.

with M_A and M_B being the molecular weights of A and B , respectively. Similar equations hold for species B .

Our objective is to develop expressions for the macroscopic fluxes of A and B in the porous medium. The macroscopic flux of A (or B) at some point of the porous medium is found by averaging over a neighborhood \mathcal{H} of the point the contribution to the macroscopic flux of all pores lying in \mathcal{H} . Domain \mathcal{H} is assumed to contain a statistically representative part of the pore network; that is, its characteristic size is considerably larger than the average pore size or length but considerably smaller than the length scale over which significant macroscopic concentration drop is observed. It is a reasonable approximation, therefore, to accept the concentration of A as constant over \mathcal{H} . This assumption does not contradict the existence of finite microscopic gradients, simply because the length of the pores is very small compared to the dimensions of \mathcal{H} . A similar assumption was employed by Gavalas and Kim (1981) and Nicholson and Petropoulos (1977) in their analyses of diffusion in capillary structures.

On the basis of the above assumption and using the fact that the diffusion flux of A is also constant along the pore—as it follows from the continuity equation for species A —we can write for the molar flow rate of A

$$\dot{N}_{Ak} = -D_{Ak}\pi r_k^2 \Delta c_{Ak} / l_k \quad (3)$$

where r_k , l_k , and Δc_{Ak} are the pore radius, the pore length, and the concentration drop of A between the two ends of pore k , respectively. A material balance with respect to A over a control volume containing only one node yields, using Eq. 3,

$$\sum_k \frac{D_{Ak}\pi r_k^2}{l_k} \Delta c_{Ak} = 0 \quad (4)$$

The summation in Eq. 4 is taken over all pores that meet at the considered node.

The assumption of approximately constant concentration throughout the network permits us to apply the effective medium theory to the transport problem described by Eq. 4, written for every node of the network, in a manner that is basically identical to that followed by the authors (Burganos and Sotirchos, 1987) for self- or trace diffusion problems. Thus, we define as pore conductance the quantity

$$g_{Ak} = D_{Ak}\pi r_k^2 / l_k$$

and we calculate an effective conductance, g_{Ae} , from

$$\int_g \frac{g - g_e}{g + \left(\frac{z}{2} - 1\right)g_e} f(g) dg = 0 \quad (5)$$

In Eq. 5 z is the coordination number of the network, assumed constant, and $f(g)dg$ is the number of pores per unit volume of the medium that have conductance g in the interval $[g, g + dg]$.

The original nonuniform pore network has approximately the same diffusional resistance with an "effective" network that is topologically identical with it but consists of pores that have a uniform conductance equal to g_{Ae} . The macroscopic diffusion

flux of A is obtained by applying the smooth field approximation, expressed for species A by

$$\Delta c_{Ak} = l_k \underline{n}_k \cdot \nabla c_A \quad (6)$$

with \underline{n}_k being the unit vector in the direction of pore k , to the effective network. The result is (see Burganos and Sotirchos, 1987, for details)

$$\underline{N}_A^{E-S} = -K g_{Ae} \left\{ \sum_k k_k l_k^2 (\underline{n}_k \underline{n}_k^T) \right\} \nabla c_A \quad (7)$$

where K is the number of pores per unit volume and k_k is the number fraction of pores of type k . The effective diffusivity tensor that is obtained using Eq. 7 in the general case of anisotropic networks is

$$\underline{\underline{D}}_{Ae}^{E-S} = K g_{Ae} \left\{ \sum_k k_k l_k^2 (\underline{n}_k \underline{n}_k^T) \right\}$$

The derivation of Eq. 5 assumes that all the nodes of the lattice used as a skeleton of the considered pore network are topologically equivalent. It is interesting to point out (Burganos and Sotirchos, 1987) that various such networks satisfy exactly the smooth field approximation if they consist of pores of the same conductance and of the same length (e.g., triangular, square, cubic, body-centered cubic, etc.). For uniform length pores, Eq. 7 yields, upon orientational averaging, the scalar effective diffusivity

$$D_{Ae}^{E-S} = \frac{1}{\tau} K g_{Ae} l_u^2 \quad (8)$$

where the tortuosity factor τ is equal to 3 unless the network is two-dimensional and the macroscopic concentration gradient is kept parallel to the plane defined by the network, in which case $\tau = 2$. For a network of pores of nonuniform length, l_u may be an effective pore length as discussed by Burganos and Sotirchos (1987). For a pore network of uniform pore length, Eq. 8 may also be written in the form

$$D_{Ae}^{E-S} = \frac{1}{\tau} \epsilon \frac{\langle D_A(r) r^2 \rangle_e}{\langle r^2 \rangle} \quad (9)$$

where ϵ is the porosity and the symbols $\langle \bullet \rangle_e$ and $\langle \bullet \rangle$ are employed to indicate effective medium average and arithmetic average values of quantity \bullet . The weight function used to obtain these averages is $R^*(r)$, with $R^*(r)dr$ being the fraction of pores with radius in the interval $[r, r + dr]$.

If the smooth field approximation is directly applied to the original, nonuniform network—that is, if it is assumed that the concentration gradient in each pore segment is equal to the projection of the macroscopic concentration gradient on the corresponding pore axis—the flux of A in a uniform length network will be given by

$$\underline{N}_A^S = -K \left\{ \sum_k k_k g_{Ak} l_k^2 (\underline{n}_k \underline{n}_k^T) \right\} \nabla c_A$$

and the orientationally averaged effective diffusivity for a network of uniform length by

$$D_{Ae}^S = \frac{1}{\tau} \epsilon \frac{\langle D_A(r)r^2 \rangle}{\langle r^2 \rangle}$$

with $D_A(r)$ as defined in Eq. 2.

Analysis of Multicomponent Diffusion

The dusty-gas model equations for multicomponent mass transport in porous media (Mason and Malinauskas, 1983) applied to a cylindrical capillary of radius r under isobaric conditions take the form (Jackson, 1977):

$$-c \nabla x_i = \sum_{j \neq i} \frac{x_j N_i - x_i N_j}{\mathcal{D}_{ij}} + \frac{N_i}{D_{Ki}(r)}; \quad i = 1, \dots, n \quad (10)$$

where c is the total concentration of the mixture, n is the number of species in the mixture, x_i is the mole fraction of component i , \mathcal{D}_{ij} is the binary molecular diffusivity of the (i, j) pair, D_{Ki} is the Knudsen diffusivity of i , and N_i is the flux of component i , which is constant along the pore axis under steady state nonreactive conditions. Macroscopic flux expressions for multicomponent diffusion are derived by applying Eq. 10 to a set of pores of the network that lie in a neighborhood \mathcal{H} of a point of the porous solid. As in the case of binary diffusion, domain \mathcal{H} is assumed to be statistically representative of a macroscopic point of the porous medium. The size of \mathcal{H} , however, is such that the concentration of each component can be considered approximately constant over it, as discussed in the previous section.

Before proceeding with the diffusion problem in the transition regime, it will be helpful and instructive to first consider the two limiting cases of Knudsen and ordinary diffusion.

Knudsen diffusion limit

Equation 10 reduces in the Knudsen regime to

$$-c \nabla x_i = \frac{N_i}{D_{Ki}}; \quad i = 1, \dots, n$$

which clearly states that diffusion of each component is independent of that of the other species, a result that is due to the absence of molecule-molecule collisions in the free flow (Knudsen) regime. Consequently, we can directly apply the EMT-SFA method outlined in the previous section to each component independently.

To this end, we define as the Knudsen conductance of species i for pore k the quantity

$$g_{Ki,k} = \frac{D_{Ki}(r_k) \pi r_k^2}{l_k}$$

and we use the effective medium theory equation, Eq. 5, to obtain the effective conductance for each species, $g_{Ki,e}(i = 1, \dots, n)$. From the proportionality of the Knudsen diffusion coefficient to the pore radius we have

$$D_{Ki}(r) = Q_i r \quad (11)$$

and, consequently,

$$g_{Ki,e} = Q_i \left\langle \frac{\pi r^3}{l} \right\rangle_e; \quad i = 1, \dots, n$$

Subsequent application of the smooth field assumption results in the following expression for the orientationally averaged effective diffusivity

$$D_{Ki,e}^{E-S} = \frac{K \langle l^2 \rangle}{\tau} Q_i \left\langle \frac{\pi r^3}{l} \right\rangle_e \quad (12a)$$

For a pore network of uniform pore length, Eq. 12a becomes

$$D_{Ki,e}^{E-S} = \frac{1}{\tau} \epsilon Q_i \frac{\langle r^3 \rangle_e}{\langle r^2 \rangle} \quad (12b)$$

Direct application of the smooth field assumption to the original network yields, for uniform pore length, an effective diffusivity equal to

$$D_{Ki,e}^S = \frac{1}{\tau} \epsilon Q_i \frac{\langle r^3 \rangle}{\langle r^2 \rangle} \quad (13)$$

Ordinary diffusion limit

In the bulk or ordinary diffusion limit Eqs. 10 reduce to the Stefan-Maxwell relations

$$-c \nabla x_i = \sum_{j \neq i} \frac{x_j N_i - x_i N_j}{\mathcal{D}_{ij}}; \quad i, j = 1, \dots, n \quad (14)$$

which are obviously coupled with respect to the fluxes N_i . Notice that only $(n - 1)$ of Eqs. 14 are independent, since

$$\sum_{i=1}^n x_i = 1$$

and $\mathcal{D}_{ij} = \mathcal{D}_{ji}$; $i, j = 1, \dots, n$. The n th equation needed for the unique determination of the N_i 's is provided by the overall momentum balance for the system. In terms of the molar flow rates in a pore k we can write

$$-c \frac{D^* \pi r_k^2}{l_k} \Delta x_{ik} = \sum_{j \neq i} \frac{x_j \dot{N}_{ik} - x_i \dot{N}_{jk}}{\mathcal{D}_{ij}/D^*}; \quad i, j = 1, \dots, n \quad (15)$$

where D^* is some arbitrarily chosen reference diffusivity (e.g., \mathcal{D}_{12}). Taking the summation of Eq. 15 for all pores meeting at a node gives

$$-\sum_k c D^* \pi r_k^2 \frac{\Delta x_{ik}}{l_k} = \sum_{j \neq i} \frac{x_j}{\mathcal{D}_{ij}/D^*} \sum_k \dot{N}_{ik} - \sum_{j \neq i} \left(\frac{x_i}{\mathcal{D}_{ij}/D^*} \sum_k \dot{N}_{jk} \right); \quad i, j = 1, \dots, n \quad (16)$$

From the material balance of each species at the node it follows that $\sum_k \dot{N}_{ik} = 0$, and hence, Eq. 16 becomes

$$\sum_k D^* \pi r_k^2 \frac{\Delta x_{ik}}{l_k} = 0; \quad i = 1, \dots, n \quad (17)$$

Equation 17 qualifies for an effective medium treatment that will replace the conductances of the various pores in the network (the same for all components)

$$g^* = \frac{D^* \pi r^2}{l}$$

by a uniform conductance, g_e^* , evaluated from the effective medium theory equation.

Macroscopic flux expressions for the pore network are obtained using the equation (Burganos and Sotirchos, 1987)

$$\underline{N}_i = K \sum_k k_k \dot{N}_{ik} l_k \underline{n}_k; \quad i = 1, \dots, n \quad (18)$$

Application of Eq. 18 to Eq. 15, written for the effective network, yields the equation

$$\sum_{j \neq i} \frac{x_j \underline{N}_i - x_i \underline{N}_j}{\mathcal{D}_{ij}/D^*} = -c g_e^* K \sum_k k_k l_k \underline{n}_k \Delta x_{ik}$$

which by using the smooth field approximation becomes

$$\sum_{j \neq i} \frac{x_j \underline{N}_i - x_i \underline{N}_j}{\mathcal{D}_{ij}/D^*} = -c g_e^* K \sum_k k_k l_k^2 (\underline{n}_k \underline{n}_k^T) \nabla x_i \quad (19)$$

By averaging Eq. 19 orientationally so as to induce isotropy to the network, we obtain the flux expressions

$$\sum_{j \neq i} \frac{x_j \underline{N}_i - x_i \underline{N}_j}{\mathcal{D}_{ij,e}^{E-S}} = -c \nabla x_i; \quad i = 1, \dots, n \quad (20)$$

where the effective binary diffusion coefficients are given by

$$\mathcal{D}_{ij,e}^{E-S} = \frac{K \langle l^2 \rangle}{\tau} \mathcal{D}_{ij} \left\langle \frac{\pi r^2}{l} \right\rangle_e \quad (21a)$$

For a network of uniform length pores, Eq. 21a takes the form (compare with Eqs. 9 and 12b)

$$\mathcal{D}_{ij,e}^{E-S} = \frac{1}{\tau} \epsilon \mathcal{D}_{ij} \frac{\langle r^2 \rangle_e}{\langle r^2 \rangle} \quad (21b)$$

Direct application of the smooth field approximation to the original network would result in the same final form of flux expressions, i.e., Eq. 20, but with pair effective diffusivities given for a network of pores of uniform length by

$$\mathcal{D}_{ij,e}^S = \frac{1}{\tau} \epsilon \mathcal{D}_{ij} \quad (22)$$

Transition diffusion regime

In the transition regime, where both Knudsen and bulk diffusional resistances are significant, Eqs. 10, written below in terms of the molar flow rates in pore k as

$$-c \frac{\pi r_k^2}{l_k} \Delta x_{ik} = \sum_{j \neq i} \frac{x_j \dot{N}_{ik} - x_i \dot{N}_{jk}}{\mathcal{D}_{ij}} + \frac{\dot{N}_{ik}}{D_{ki,k}}; \quad i = 1, \dots, n, \quad (23)$$

cannot admit a direct effective medium treatment, because of the pore radius dependence of the Knudsen diffusion coefficients that appear in the righthand side.

This problem can be overcome by decoupling the system of flux expressions given by Eq. 23 via a series of matrix manipulations, which exploit the special structure of the dusty-gas model flux expressions, into a set of n independent equations, each of which can then be treated using the EMT-SFA procedure or, in fact, any other averaging procedure applicable. To this end, we multiply Eq. 23 by $\alpha_i = Q_i/Q^*$, with Q_i as defined in Eq. 11 and Q^* a reference value, and write the result in matrix form for $i = 1, \dots, n$ to get

$$-c \frac{\pi r_k^2}{l_k} \begin{pmatrix} \alpha_1 \Delta x_{1k} \\ \alpha_2 \Delta x_{2k} \\ \vdots \\ \alpha_n \Delta x_{nk} \end{pmatrix} = \begin{pmatrix} \frac{1}{Q^* r_k} + \alpha_1 \sum_{i \neq 1} \frac{x_i}{\mathcal{D}_{1i}} & \frac{-\alpha_1 x_1}{\mathcal{D}_{12}} & \dots & \frac{-\alpha_1 x_1}{\mathcal{D}_{1n}} \\ \frac{-\alpha_2 x_2}{\mathcal{D}_{12}} & \frac{1}{Q^* r_k} + \alpha_2 \sum_{i \neq 2} \frac{x_i}{\mathcal{D}_{2i}} & \dots & \frac{-\alpha_2 x_2}{\mathcal{D}_{2n}} \\ \vdots & \vdots & \ddots & \vdots \\ \frac{-\alpha_n x_n}{\mathcal{D}_{1n}} & \frac{-\alpha_n x_n}{\mathcal{D}_{2n}} & \dots & \frac{1}{Q^* r_k} + \alpha_n \sum_{i \neq n} \frac{x_i}{\mathcal{D}_{ni}} \end{pmatrix} \begin{pmatrix} \dot{N}_{1k} \\ \dot{N}_{2k} \\ \vdots \\ \dot{N}_{nk} \end{pmatrix}$$

or in matrix notation

$$-\frac{\pi r_k^2}{l_k} \Delta y_k = T \dot{N}_k \quad (24)$$

Notice that the only dependence of T on the pore radius is the term $1/Q^* r_k$ that appears in its diagonal elements. Therefore, if B is the corresponding matrix in the bulk problem, we obviously

have

$$T = B + \frac{1}{Q^* r_k} I \quad (25)$$

with I being the unit matrix. It follows from Eq. 25 that the eigenvalues η_i of T can be related to the eigenvalues λ_i of B

through

$$\eta_i = \lambda_i + \frac{1}{Q^* r_k}; \quad i = 1, \dots, n$$

and that T and B have the same eigenvectors, that is, the eigenvectors of T are independent of the pore radius, r .

If we denote by Z the matrix that is made up of the eigenvectors of B , we can write Eq. 24 in the form

$$-\Delta y_k = Z \Lambda Z^{-1} \dot{N}_k \quad (26)$$

where $\Lambda = \text{diag} [(\lambda_i + 1/Q^* r_k) l_k / \pi r_k^2; i = 1, \dots, n]$. Premultiplying Eq. 26 by Z^{-1} gives

$$-\Delta w_k = \Lambda \dot{M}_k$$

with the elements of the vectors $\Delta w_k = Z^{-1} \Delta y_k$ and $\dot{M}_k = Z^{-1} \dot{N}_k$ being linear, pore radius independent combinations of the concentration drops and the flow rates in the pore, respectively. Notice that for the i th element of these vectors we have that

$$-\frac{1}{\left(\lambda_i + \frac{1}{Q^* r_k}\right) \frac{l_k}{\pi r_k^2}} \Delta w_{ik} = \dot{M}_{ik} \quad (27)$$

Equation 27 prompts us to define n auxiliary species with the i th species having, in pore k , "flow rate" \dot{M}_{ik} , "concentration drop" Δw_{ik} , and "conductance" $[(\lambda_i + 1/Q^* r_k) l_k / \pi r_k^2]^{-1}$. Such a definition becomes meaningful when one notices that these auxiliary components satisfy the material balance equation at any node, since their "flow rates" are linear and pore-independent combinations of the flow rates of the real components. Moreover, the eigenvalues of B are real and nonnegative (a proof based on thermodynamics arguments was given by Stewart and Prober, 1964, while a mathematical proof is presented in Appendix A), and hence the physical term "conductance" can be used for the above quantity. Application of the EMT to the n auxiliary species yields n "effective conductances" given by

$$g_{ie} = \left\langle \frac{1}{\left(\lambda_i + \frac{1}{Q^* r}\right) \frac{l}{\pi r^2}} \right\rangle_e; \quad i = 1, \dots, n \quad (28)$$

Using the "effective conductances" given by Eq. 28, eq. 26 becomes

$$-\Delta y_k = Z \Lambda_e Z^{-1} \dot{N}_k \quad (29)$$

where

$$\Lambda_e = \text{diag} \left(\frac{1}{g_{1e}}, \frac{1}{g_{2e}}, \dots, \frac{1}{g_{ne}} \right)$$

The following macroscopic flux expressions are obtained from Eq. 29 by use of Eq. 18 and subsequent application of the

smooth field approximation, Eq. 6:

$$-cK \sum_k k_k l_k^2 (\underline{n}_k \underline{n}_k^T) \nabla x = A^{-1} Z \Lambda_e Z^{-1} \underline{N} \quad (30)$$

where $A = \text{diag}(\alpha_1, \alpha_2, \dots, \alpha_n)$. Orientational averaging of Eq. 30, followed by some rearrangement, finally leads to the flux relations

$$-c \nabla x = A^{-1} Z (D_e^{E-S})^{-1} Z^{-1} \underline{N} \quad (31)$$

where $D_e^{E-S} = \text{diag} (K \langle l^2 \rangle g_{ie} / \tau; i = 1, \dots, n)$. For a network of pores of uniform length, the elements of matrix D_e^{E-S} become equal to

$$D_{ie}^{E-S} = \frac{1}{\tau} \epsilon \frac{\left\langle \frac{1}{\lambda_i + \frac{1}{Q^* r^3}} \right\rangle_e}{\langle r^2 \rangle} \quad (32)$$

It should be emphasized that the accuracy of the diffusion flux relations given by Eqs. 30 and 31 for a pore network whose effective network satisfies exactly the smooth field approximation (e.g., the uniform pore length networks discussed earlier), depends only on the effective medium theory since no other assumptions were employed in their derivation. Previous extensive computations by the authors (Burganos and Sotirchos, 1987) for square and cubic pore networks showed that effective diffusivities and diffusion fluxes computed by the EMT-SFA procedure as applied to self- or trace diffusion are in excellent agreement with those resulting from the exact solution of the mass transport problem in these networks for all types of pore size distributions considered. This is also expected to be the case for the multicomponent flux expressions derived since each of the n independent transport subproblems to which the EMT-SFA procedure was applied (see Eq. 27) is qualitatively equivalent to the transport problem for single-species diffusion.

If the smooth field approximation is directly applied to Eq. 27, the resulting flux expressions are of the same form as Eqs. 30 and 31, the only difference being that the arithmetic mean of conductance g_i, \hat{g}_i , appears in the flux expressions instead of the effective medium average, g_{ie} . For instance, Eq. 31 is written:

$$-c \nabla x = A^{-1} Z (D_e^S)^{-1} Z^{-1} \underline{N} \quad (33)$$

where $D_e^S = \text{diag} (K \langle l^2 \rangle \hat{g}_i / \tau; i = 1, \dots, n)$. For a network of pores of uniform length, the elements of matrix D_e^S are given by

$$D_{ie}^S = \frac{1}{\tau} \epsilon \frac{\left\langle \frac{1}{\lambda_i + \frac{1}{Q^* r^3}} \right\rangle_e}{\langle r^2 \rangle} \quad (34)$$

The multicomponent flux expressions obtained by direct application of the smooth field approximation to the original network are in a final analysis equivalent to those derived by Feng and Stewart (1973). However, the flux relations developed here exploit the special structure of the dusty-gas model equations, and thus they require averaging of only n quantities, namely the g_i 's, over the pore size, pore length, and pore orientation distri-

butions. However, the diffusion flux expressions derived by Feng and Stewart involve, as applied to isobaric diffusion, inversion of an $(n-1) \times (n-1)$ matrix (since the $n \times n$ matrix is singular) and subsequent averaging of all elements of the inverse matrix over the pore size and orientation distributions.

Approximate Analysis of Multicomponent Diffusion in the Transition Regime

The diffusion flux expressions derived in the previous section, though rigorous, have the practical disadvantage of requiring the computation of n concentration-dependent eigenvalues and eigenvectors. Therefore, every time the concentration data in the pore network are altered, the whole sequence of computations leading to Eq. 31 (or Eq. 33 for the SFA approximation) has to be repeated. In a problem with both temporally and spatially evolving characteristics this means that the above computations have to be carried out for every spatial or temporal discretization point. A set of approximate flux expressions will be developed in the following paragraphs which, although they involve minimal computational effort for their implementation, yield results comparable to those of the rigorous EMT-SFA and SFA approximations, Eqs. 31 and 33, respectively.

Using simple momentum-transfer arguments, the concentration gradient of species i in a pore can be considered to be made up (Mason and Malinauskas, 1983) of separate contributions for the Knudsen diffusional limitations (molecule-wall collisions) and for the molecular diffusional limitations (molecule-molecule collisions). For the concentration gradient of species i in pore k , for instance, we write

$$\nabla x_{ik} = \nabla x_{ik}^B + \nabla x_{ik}^K; \quad i = 1, \dots, n$$

where

$$\begin{aligned} -c \nabla x_{ik}^K &= \frac{N_{ik}}{D_{Ki,k}}; \quad i = 1, \dots, n \\ -c \nabla x_{ik}^B &= \sum_{j \neq i} \frac{x_j N_{jk} - x_i N_{kj}}{D_{ij}}; \quad i, j = 1, \dots, n \end{aligned}$$

If we assume that the same momentum-transfer arguments also apply to the macroscopic diffusion problem, i.e.,

$$\nabla x_i = \nabla x_i^B + \nabla x_i^K; \quad i = 1, \dots, n \quad (35)$$

we can completely dissociate the Knudsen diffusion problem from the molecular diffusion problem and apply the EMT-SFA procedure to each one independently. Indeed, working as explained above we obtain for the orientationally averaged diffusion fluxes the expressions

$$-c \nabla x_i^K = \frac{N_i}{D_{Ki,e}^{E-S}}; \quad i = 1, \dots, n \quad (36)$$

$$-c \nabla x_i^B = \sum_{j \neq i} \frac{x_j N_j - x_i N_i}{D_{ij,e}^{E-S}}; \quad i, j = 1, \dots, n \quad (37)$$

with $D_{Ki,e}^{E-S}$ and $D_{ij,e}^{E-S}$ given by Eqs. 12a and 21a. Equations 36 and 37 combined with Eq. 35 lead to the macroscopic flux

expressions

$$-c \nabla x_i = \sum_{j \neq i} \frac{x_j N_j - x_i N_i}{D_{ij,e}^{E-S}} + \frac{N_i}{D_{Ki,e}^{E-S}}; \quad i, j = 1, \dots, n \quad (38)$$

Equations 38 are obviously considerably simpler than the flux expressions obtained through rigorous application of the EMT-SFA procedure. They retain the form of the dusty-gas model equations, and the effective diffusion coefficients employed in them are independent of the species concentration and need not be updated as the macroscopic concentration fields evolve spatially or temporally. However, the question is how well, both qualitatively and quantitatively, the approximate flux relations can follow the predictions of the rigorous EMT-SFA flux expressions.

In order to facilitate the comparison of the two flux models, we recast Eq. 38 in a form similar to that of Eq. 31. To this end, we write Eqs. 38 in matrix form, multiply the righthand side of the resulting expression by $A^{-1}A$, and use Eqs. 12a and 21a for $D_{Ki,e}^{E-S}$ and $D_{ij,e}^{E-S}$, respectively, to obtain

$$-c \nabla x = A^{-1} Z (D_e^{E-S})^{-1} Z^{-1} N \quad (39)$$

where the elements of the diagonal matrix D_e^{E-S} are given by

$$D_{ie}^{E-S} = \frac{K \langle l^2 \rangle}{\tau} \left[\frac{1}{\frac{\lambda_i}{\pi r^2} + \frac{1}{Q^* \pi r^3}} \right]; \quad i = 1, \dots, n$$

Comparison of Eq. 39 with Eq. 31 reveals that the deviation of the predictions of the approximate EMT-SFA flux expressions from those of the rigorous ones depends solely on how well the elements of matrix D_e^{E-S} approximate those of matrix D_e^{E-S} , that is, on the accuracy of the approximation

$$\left\langle \frac{1}{\frac{\lambda_i}{\pi r^2} + \frac{1}{Q^* \pi r^3}} \right\rangle_e \approx \frac{1}{\frac{\lambda_i}{\langle \pi r^2 \rangle_e} + \frac{1}{\langle Q^* \pi r^3 \rangle_e}}; \quad i = 1, \dots, n \quad (40)$$

For a network of pores of uniform length, Eq. 40 takes the form

$$\left\langle \frac{1}{\frac{\lambda_i}{r^2} + \frac{1}{Q^* r^3}} \right\rangle_e \approx \frac{1}{\frac{\lambda_i}{\langle r^2 \rangle_e} + \frac{1}{Q^* \langle r^3 \rangle_e}}; \quad i = 1, \dots, n \quad (41)$$

which will be discussed in detail in the following paragraphs.

The approximate method of multicomponent analysis can also be followed in the case when the SFA approximation is directly applied to the pore network. The obtained flux models have the form

$$-c \nabla x_i = \sum_{j \neq i} \frac{x_j N_j - x_i N_i}{D_{ij,e}^S} + \frac{N_i}{D_{Ki,e}^S}; \quad i, j = 1, \dots, n \quad (42)$$

with the effective Knudsen and binary molecular diffusivities given, for a uniform length network, by Eqs. 13 and 22. Equations

tion 42 may be written in a form similar to that of Eq. 33 by following the procedure outlined above for Eq. 38. Comparison of the resulting flux expression with that obtained through rigorous application of the smooth field approximation, Eq. 33, shows that the deviation depends, for a uniform pore network, on the accuracy of the approximation

$$\left\langle \frac{1}{\frac{\lambda_i}{r^2} + \frac{1}{Q^* r^3}} \right\rangle \approx \frac{1}{\frac{\lambda_i}{\langle r^2 \rangle} + \frac{1}{Q^* \langle r^3 \rangle}}; \quad i = 1, \dots, n \quad (43)$$

which will also be examined next.

It is interesting to note that the macroscopic fluxes as computed by the rigorous as well as the approximate EMT-SFA model satisfy Graham's law for isobaric mixtures. The same is true for the flux expressions resulting from the rigorous and approximate application of the SFA to the original pore network. Indeed, using Eqs. 12, 21, and 38 one can show that Graham's law is satisfied when the approximate form of the EMT-SFA model is used and analogous is the proof for the approximate application of the SFA method. However, in the case of the rigorous EMT-SFA and SFA flux models the proof is not so obvious but requires some matrix manipulations, which are presented in Appendix B.

It is clear from the form of Eqs. 32, 34, 41, and 43 that $(\lambda_i Q^*)$ functions as the weight factor of the contribution of the mechanism of ordinary diffusion to the diffusion process of the i th auxiliary component. Therefore, it is possible by varying $(\lambda_i Q^*)$ from zero to infinity to investigate the accuracy of Eqs. 41 and 43 over the whole diffusion range from the Knudsen regime $[(\lambda_i Q^*) = 0]$ to the molecular regime $[(\lambda_i Q^*) \rightarrow \infty]$. At the two limits, the approximations given by Eqs. 41 and 43 obviously hold as identities.

The accuracy of the above approximations in the transition regime is numerically investigated in the following paragraphs for a discrete bimodal pore system of uniform-length pores, which offers the simplest possible representation of a distributed pore size solid. The number density function $R(r)$ for such a system is obviously given by

$$R(r) = f_1 \delta(r - r_1) + f_2 \delta(r - r_2) \quad (44)$$

where f_i is the number of pores per unit volume with radius r_i . The corresponding porosity density function

$$\epsilon(r) = \epsilon_1 \delta(r - r_1) + \epsilon_2 \delta(r - r_2)$$

is related to $R(r)$, for insignificant volume of pore overlap at the nodes, by the relation

$$\epsilon_i = f_i \pi r_i^2 l_u; \quad i = 1, 2 \quad (45)$$

Figure 2 compares the elements of the diagonal matrices D_e^{E-S} and D_e^{E-S} (or equivalently the two sides of Eq. 41) over a wide range of $(\lambda_i Q^*)$ for a pore network with coordination number equal to 4 and $r_1/r_2 = 10$ with the population ratio $\alpha = f_1/f_2$ as a parameter. The solid curves represent the elements of D_e^{E-S} (lefthand side of Eq. 41), while the dashed curves represent the elements of the approximate matrix (righthand side of Eq. 41). The effective diffusivity values used in the figure have been rendered dimensionless by using the effective diffusivity at the

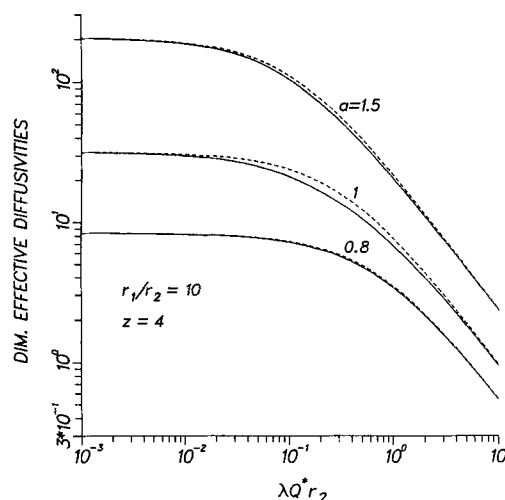


Figure 2. Effective diffusivities obtained by EMT-SFA method for the auxiliary components in a network.

$z = 4$; discrete bimodal distribution of pore size ($r_1/r_2 = 10$) over entire diffusion regime
— Rigorous application of method; ---- approximate procedure

Knudsen limit and for $\alpha = 0$ as a reference value. The dimensionless group $(\lambda_i Q^* r_2)$ was used as the abscissa in the figure in order to make the results shown independent of the actual values of r_1 and r_2 . The results of Figure 2 show that the approximate effective diffusivities of the auxiliary components approximate satisfactorily those obtained through rigorous application of the EMT-SFA procedure. It must be mentioned that the values of α , z , and r_1/r_2 used in the figure have been chosen so as to obtain the largest possible deviations. Similar results have been obtained using discrete multimodal distributions of pore size. It is thus believed that the approximation expressed by Eq. 41 can be

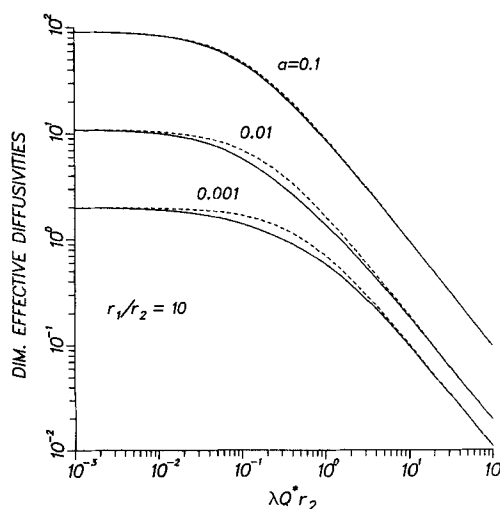


Figure 3. Effective pore conductances obtained by SFA method for the auxiliary components in a network.

$z = 4$; discrete bimodal distribution of pore size ($r_1/r_2 = 10$) over entire diffusion regime
— Rigorous application of method; ---- approximate procedure

considered satisfactory for most types of pore size distribution used in practice.

Similar conclusions have been reached for the effective diffusivities obtained by direct application of the smooth field approximation to the original network, Figure 3. The elements of the diagonal diffusivity matrix D_e^S (solid curves) are satisfactorily approximated by those of the approximate matrix D_e^{S*} (see Eq. 43). However, the maximum deviations occur at much lower values of the population ratio α than in the case of the EMT-SFA model (compare Figures 2 and 3). It can be shown (Burganos, 1987) that the approximate effective diffusivities are always greater than the exact diffusivities, in accord with the results shown in Figure 3.

Application to Ternary Gas Diffusion in a Porous Pellet

The various flux models developed in the previous section are applied here to the isobaric diffusion of a ternary mixture of H_2 , N_2 , and CO_2 in a porous solid whose pore structure is assumed to be represented by a cubic pore network ($z = 6$). The computed results are used to compare the predictions of the rigorous and approximate EMT-SFA and SFA flux models. We chose to work with the above gaseous species because of their largely different molecular weights and, hence, Knudsen and binary diffusion coefficients. At atmospheric pressure and 293 K temperature, the molecular diffusivities are taken equal to $\mathcal{D}_{H_2, N_2} = 0.739 \text{ cm}^2/\text{s}$, $\mathcal{D}_{H_2, CO_2} = 0.616 \text{ cm}^2/\text{s}$, and $\mathcal{D}_{N_2, CO_2} = 0.147 \text{ cm}^2/\text{s}$ (Hirschfelder et al., 1954). We further assume a discrete bimodal pore size distribution for the solid and uniform pore length (see Eqs. 44–45). As mentioned before (see also Burganos and Sotirchos, 1987), however, the latter assumption is not necessary for the application of the flux models developed.

We consider a slab of a porous solid with its two parallel faces \mathcal{S}_1 and \mathcal{S}_2 located at distance L from each other. The mole fractions of the components of the ternary mixture are maintained at constant values over \mathcal{S}_1 and \mathcal{S}_2 , and consequently the diffusion problem considered is essentially one-dimensional in the direction perpendicular to \mathcal{S}_1 and \mathcal{S}_2 , the z direction. Equations 31 and 33 are written

$$-c \begin{pmatrix} dx_1/dz \\ dx_2/dz \\ dx_3/dz \end{pmatrix} = A^{-1} Z (D_e^{E-S} \text{ or } D_e^S)^{-1} Z^{-1} \begin{pmatrix} N_1 \\ N_2 \\ N_3 \end{pmatrix} \quad (46)$$

with $N_i = \text{constant}$ ($i = 1, 2, 3$), as required by the species continuity equations. The matrix of the eigenvectors of B , Eq. 25, Z , and the eigenvalues of B are concentration-dependent and therefore have to be computed for every set of mole fraction values. For a ternary mixture, however, it is possible to derive analytic expressions for the eigenvectors and eigenvalues of B . The eigenvalues are used in the computation, using Eq. 32 or 34, of the effective diffusivity of the auxiliary components, i.e., the elements of the diagonal matrix D_e^{E-S} or D_e^S . Equations 46 were solved for the mole fractions, x_i , and the constant fluxes, N_i , using a B-spline collocation scheme (de Boor, 1978). The constant values of x_i at the two faces of the porous slab, \mathcal{S}_1 and \mathcal{S}_2 , were used to complement Eqs. 46 as boundary conditions.

If the approximate EMT-SFA or SFA flux expressions are

used, Eq. 46 takes the form

$$\frac{dx}{dz} = C(N)x + b(N) \quad (47)$$

where the elements of matrix $C(N)$ and vector $b(N)$ are linear combinations of the fluxes. Using the eigenvector-eigenrow formalism, Eq. 47 may be solved analytically to get in general form

$$x = b_1(x_0, N) + b_2(x_0, N) \exp[-\mu_2(N)z] + b_3(x_0, N) \exp[-\mu_3(N)z]$$

where x_0 is the vector of mole fractions at $z = 0$, $b_i(x_0, N)$ are vectors whose elements depend on x_0 and N , and μ_i are the eigenvalues of $C(N)$. The vector of fluxes, N , is determined by forcing x to satisfy the boundary conditions at $z = L$.

The diffusion fluxes predicted by the rigorous EMT-SFA and SFA models are compared in Figure 4. The ordinary diffusion limit was obtained by assigning large values to the pore sizes r_1 and r_2 , while smaller values gave the results corresponding to the transition and Knudsen regimes. The results of Figure 4 were obtained for

$$[x_{H_2}, x_{N_2}, x_{CO_2}] = \begin{cases} [0.1, 0.2, 0.7]; & z = 0 \\ [0.9, 0.1, 0.0]; & z = L \end{cases}$$

At the Knudsen or bulk diffusion limit, all diffusion flux ratios, (N_i^{E-S}/N_i^S) , are equal since the D_e^{E-S}/D_e^S ratios are also equal (see Eqs. 12, 13, 21, and 22). Actually the two limiting curves of Figure 4 can be constructed by simply plotting the ratios $\langle r^2 \rangle_e / \langle r^2 \rangle$ (bulk) and $\langle r^3 \rangle_e / \langle r^3 \rangle$ (Knudsen). As the results of Figure 4 show, the diffusion flux ratios of the three species are very close to each other in the transition regime as well. The reason for this behavior lies in the fact that since two nonzero eigenvalues of

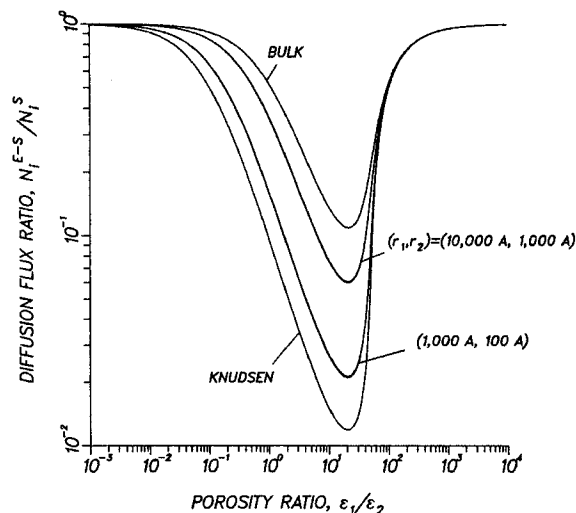


Figure 4. Ratio of magnitudes of fluxes for components of a ternary mixture as predicted by EMT-SFA and SFA methods vs. porosity ratio for a discrete bimodal system of pores forming a cubic network.

matrix B are close to each other, the corresponding D_{ie}^{E-S}/D_{ie}^S ratios differ only slightly. The diffusivity ratio corresponding to the zero eigenvalue is significantly different but since the eigenvector of B that corresponds to it is orthogonal to $A\nabla x$ (for isobaric diffusion), its value does not appear in the computation of the fluxes. This is the reason only one effective diffusivity is encountered in the earlier analysis of the binary system.

The results of Figure 4 clearly show that direct application of the smooth field approximation to the pore network leads to marked overestimation of the diffusion fluxes in the pore network. This observation agrees with the results reported by Burganos and Sotirchos (1987) for trace diffusion in pore networks. It was pointed out there that the diffusion coefficients obtained by application of the SFA procedure—which violates the mass balance equations at the nodes—correspond to in-parallel combination of the diffusional resistances of the pores in the network. On the other hand, the EMT-SFA procedure yields effective diffusion coefficients which for coordination number equal to 2 correspond to in-series combination of the diffusional resistances of the pores, while for other coordination numbers a situation intermediate to combination of the diffusional resistances in parallel and in series obtains. This is exactly the reason that the SFA predictions are always higher than the EMT-SFA predictions. It is seen in Figure 4 that the diffusion coefficients predicted by the smooth field approximation procedure are, in some cases, higher than those based on the EMT-SFA procedure by more than one order of magnitude. This could very well be the reason that flux models based on the smooth field approximation require tortuosity factors larger than 3 in order to provide a good approximation to experimental diffusion data (Satterfield, 1970).

The mole fraction profiles for the (H_2 , N_2 , CO_2) mixture predicted by the rigorous EMT-SFA and SFA flux models are shown in Figure 5 for a solid with $r_1/r_2 = 10$ and $\epsilon_1/\epsilon_2 = 10$. The profiles obtained at the bulk and Knudsen diffusion limits are also shown in the figure. Since the effective diffusivities predicted by the two methods are proportional to each other in the

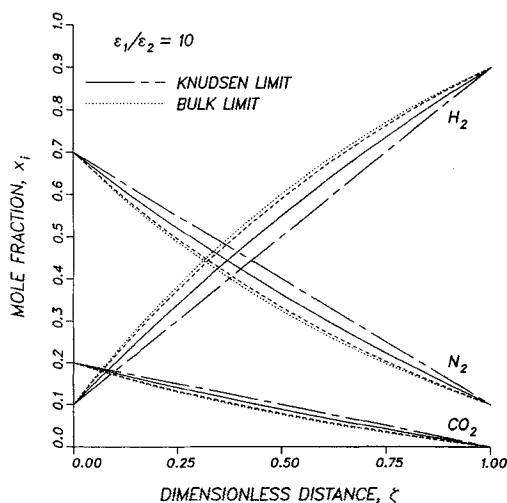


Figure 5. Concentration profiles for components of a ternary mixture diffusing in a cubic pore network for discrete bimodal pore size distribution ($r_1 = 10,000\text{\AA}$, $r_2 = 1,000\text{\AA}$)
— EMT-SFA predictions; ---- SFA predictions

Knudsen and bulk diffusion regimes, the mole fraction profiles are the same although the diffusion fluxes are different, Figure 4. Notice that the mole fraction profiles predicted by the EMT-SFA method are closer to those of the Knudsen diffusion regime, a consequence of the fact that the EMT-SFA procedure places more weight on the diffusional resistance of the small pores.

The predictions of the rigorous EMT-SFA and SFA procedures are compared in Figures 6 and 7 with those based upon the corresponding approximate models developed in the previous section. In order to avoid mentioning specific values for the pellet length and porosity, we chose to plot the quantities $N_i L/\epsilon$ instead of the fluxes. We again tried to appropriately choose the values of the parameters so as to obtain the largest possible deviations. The results in Figure 6 clearly show that the approximate flux model for the EMT-SFA procedure performs successfully, leading to hardly noticeable deviations. Somewhat larger deviations are observed in the comparison of the SFA models, Figure 7, but taking into account the considerably larger numerical effort involved in the application of the rigorous model, the approximate SFA model must also be considered successful. For obvious reasons (see Eqs. 41 and 43), when either pore size dominates the pore population, the rigorous and approximate models give the same results.

Conclusions

The problem of multicomponent, isobaric diffusion in porous structures have been considered, and flux models have been developed for pore networks of distributed pore size and length constructed by arranging pore segments around the bonds of a two- or three-dimensional lattice of constant coordination number. The dusty-gas model equations were used to describe the diffusion process in each pore segment, and a sequence of matrix manipulations was used to uncouple them into a set of n independent flux expressions defined for n auxiliary species. Each single-species flux expression was then treated using the EMT-SFA procedure developed by the authors in a previous paper (Burganos and Sotirchos, 1987), which consists in using the

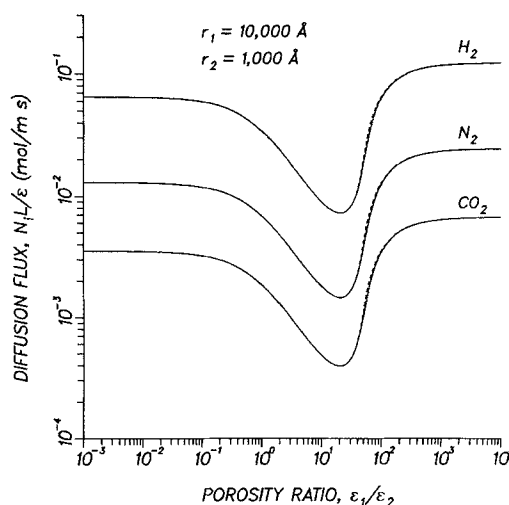


Figure 6. Dependence of quantity NL/ϵ for components of mixture of Figure 5 as predicted by EMT-SFA method on porosity ratio.
— Rigorous application of method; ---- approximate procedure

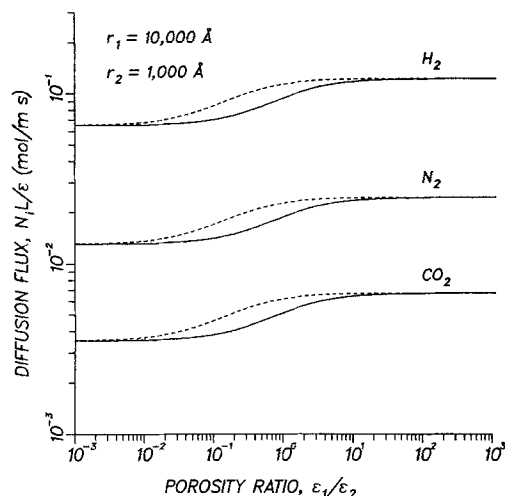


Figure 7. Dependence of quantity NL/ϵ for components of mixture of Figure 5 as predicted by SFA method on porosity ratio.

— Rigorous application of method; ---- approximate procedure

effective medium theory for resistor networks to replace the original network by an equivalent, with respect to mass transport resistance, network of uniform conductance that is further analyzed using the smooth field approximation. The analysis used in the development of the flux expressions is local in the sense that the macroscopic diffusion flux is obtained by averaging the contributions of all pores lying in a statistically representative part of the network whose characteristic size is assumed to be much smaller than the length scale associated with significant macroscopic concentration differences.

In addition to the flux model developed using the above procedure, we also constructed an approximate model by assuming that the concentration drop in each pore and in the porous medium can be divided into separate Knudsen and molecular diffusion contributions, thus making it possible to treat the Knudsen and molecular diffusion problems independently of each other. The main advantage of the approximate flux expressions over the rigorous ones stems from the fact that the former retain the form of the dusty-gas model equations and, as a result, the effective diffusivities employed in them are independent of the mole fractions. Our numerical computations revealed small differences between the effective diffusivities of the auxiliary components for discrete, multimodal pore size distributions obtained through rigorous application of the EMT-SFA procedure and those resulting from the corresponding approximate model. A similar relation was found to hold between the effective diffusivities of the rigorous and approximate model obtained through direct application of the smooth field approximation to the original network.

The above observations were further verified by applying the developed flux models to study the diffusion of a ternary mixture of H_2 , N_2 , and CO_2 in a porous slab. Our numerical results also showed that direct application of the smooth field approximation underestimates severely the diffusional resistance in the pore network, a conclusion that is in qualitative agreement with our previous results for trace diffusion (Burganos and Sotirchos, 1987). Numerical computations presented in our previous work showed that the EMT-SFA procedure yields effective diffusion

coefficients that are almost identical to those obtained by direct solution of the transport equation in the network for various pore size distributions. This must also be true for the predictions of the multicomponent EMT-SFA flux expressions developed in the present study since each of the n independent diffusion problems used in their derivation is qualitatively identical to that for trace diffusion.

Acknowledgment

Acknowledgment is made to the Donors of the Petroleum Research Fund, administered by the American Chemical Society, for partial support of this research. This research was also supported in part by a grant from the U.S. Department of Energy.

Notation

- A = diagonal matrix, Eq. 30
- B = matrix, Eq. 25
- c = concentration of mixture
- c_i = concentration of species i
- d = dimensionality of network
- D^* = reference diffusivity
- \underline{D}_{Ae} = effective diffusivity tensor for species A (binary mixture)
- D_{Ak}, \bar{D}_{Ae} = diffusion coefficient of species A in pore k , effective diffusion coefficient of species A (binary mixture)
- D_e = diagonal matrix of effective diffusivities of auxiliary components
- D_{ie} = effective diffusivity of i th auxiliary species
- $D_{ij}, \bar{D}_{ij,e}$ = binary diffusivity of (i, j) pair, effective binary diffusivity
- D_{Kik}, D_{Kie} = Knudsen diffusivity of species i in pore k , effective Knudsen diffusivity of species i
- $f(g)dg$ = number of pores per unit volume with conductance in range $[g, g + dg]$
- f_i = number of pores per unit volume with conductance g_i in a network with discrete distribution of conductance or pore size
- g = conductance of a pore
- g^*, g_e^* = conductance of a pore with diffusivity D^* , effective conductance
- g_{Ak}, g_{Ae} = conductance of pore k for species A , effective conductance (binary mixture)
- g_{ie} = effective conductance of auxiliary species i
- g_{Kik}, g_{Kie} = Knudsen conductance of species i in pore k , effective Knudsen conductance of species i
- k_k = number fraction of pores of type k
- K = total number of pores per unit volume
- l = length of a pore
- l_u = pore length in a network of pores of uniform length
- M_i = molecular weight of species i
- \bar{M}_{ik} = flow rate of auxiliary species i in pore k
- \bar{M}_k = vector of flow rates of auxiliary species in pore k
- n = number of species in mixture
- n_k = unit vector parallel to axis of pore k
- \bar{N} = vector of macroscopic diffusion fluxes of mixture components
- \bar{N}_i = macroscopic diffusion flux of species i
- \bar{N}_{ik} = diffusion flux of species i in pore k
- \bar{N}_{ik} = rate of molar flow of species i in pore k
- \bar{N}_k = vector of component molar flow rates in pore k
- Q_i = Knudsen proportionality constant for species i , Eq. 11
- Q^* = reference value for Q_i
- r = pore radius
- $R(r)dr$ = number of pores per unit volume with radius in range $[r, r + dr]$
- x_i = mole fraction of species i
- x = vector of mole fractions for mixture
- z = coordination number
- Z = matrix of eigenvectors of matrix B

Greek letters

- α = population ratio in a discrete bimodal pore system
- α_i = dimensionless Knudsen proportionality constant for species i ($= Q_i/Q^*$)

Δc_{ik} = concentration difference for species i between the two ends of pore k
 Δw_{ik} = concentration drop along pore k for auxiliary species i
 Δw_k = vector of concentration drops for pore k
 Δx_{ik} = mole fraction difference for species i between the two ends of pore k
 ∇c_i = macroscopic concentration gradient for species i
 ∇c_{ik} = concentration gradient for species i in pore k
 ∇x_i = macroscopic mole fraction gradient for species i
 ∇x_{ik} = mole fraction gradient for species i in pore k
 ϵ = porosity
 $\epsilon(r)dr$ = porosity of pores with radius in range $[r, r + dr]$
 ϵ_i = porosity of pores of radius r_i in a network with discrete distribution of pore size
 λ_i = i th eigenvalue of matrix B
 Λ = diagonal matrix, Eq. 26
 τ = tortuosity factor

Subscripts

e = effective conductances obtained using Eq. 5 or effective quantities
 i = quantities referring to species i or to i th pore size of a discrete pore size distribution
 k = quantities referring to pore segment k
 ik = quantities for species i referring to pore segment k

Superscripts

$E - S$ = quantities obtained using EMT-SFA method
 S = quantities obtained using SFA method

Symbols

$\langle \cdot \rangle$ = arithmetic average value of quantity
 $\langle \cdot \rangle_e$ = effective medium average value of quantity

Appendix A: Nature of the Eigenvalues of Matrix B

We show here that the matrix

$$B = \begin{pmatrix} \alpha_1 \sum_{i \neq 1} \frac{x_i}{\mathcal{D}_{1i}} & \frac{-\alpha_1 x_1}{\mathcal{D}_{12}} & \dots & \frac{-\alpha_1 x_1}{\mathcal{D}_{1n}} \\ \frac{-\alpha_2 x_2}{\mathcal{D}_{12}} & \alpha_2 \sum_{i \neq 2} \frac{x_i}{\mathcal{D}_{2i}} & \dots & \frac{-\alpha_2 x_2}{\mathcal{D}_{2n}} \\ \vdots & \vdots & \ddots & \vdots \\ \frac{-\alpha_n x_n}{\mathcal{D}_{1n}} & \frac{-\alpha_n x_n}{\mathcal{D}_{2n}} & \dots & \alpha_n \sum_{i \neq n} \frac{x_i}{\mathcal{D}_{ni}} \end{pmatrix}$$

has nonnegative eigenvalues. The procedure followed is similar to that given by Amundson (1966) for proving that the coefficient matrix resulting from complex reaction networks that satisfy the principle of microscopic reversibility has nonpositive eigenvalues.

It can easily be shown that matrix B is self-adjoint with respect to the inner product

$$x \cdot y = x^T X y \quad (\text{A1})$$

where $X = \text{diag}(1/\alpha_1 x_1, 1/\alpha_2 x_2, \dots, 1/\alpha_n x_n)$. This states that the matrix has real eigenvalues.

To prove that the matrix has nonnegative eigenvalues, we prove that B is positive semidefinite with respect to the above

inner product, i.e., we show that

$$y^T X (B y) \geq 0 \quad (\text{A2})$$

We have that

$$F = y^T X (B y) = - \sum_{i=1}^n y_i \sum_{j=1}^n \frac{y_j}{\mathcal{D}_{ij}} \quad (\text{A3})$$

where

$$\frac{x_i}{\mathcal{D}_{ii}} = - \sum_{j=1, j \neq i}^n \frac{x_j}{\mathcal{D}_{ij}} \quad (\text{A4})$$

Introducing Eq. A4 in Eq. A3 gives

$$F = - \sum_{i=1}^n \sum_{j=1, j \neq i}^n \frac{x_i x_j}{\mathcal{D}_{ij}} \left[\frac{y_i}{x_i} \left(\frac{y_j}{x_j} - \frac{y_i}{x_i} \right) \right] \quad (\text{A5})$$

Rearranging Eq. A5 we obtain that

$$F = \sum_{i=1}^n \sum_{j=1, j \neq i}^n \frac{x_i x_j}{\mathcal{D}_{ij}} \left(\frac{y_i}{x_i} - \frac{y_j}{x_j} \right)^2 - F$$

or

$$F = \frac{1}{2} \sum_{i=1}^n \sum_{j=1, j \neq i}^n \left[\frac{x_i x_j}{\mathcal{D}_{ij}} \left(\frac{y_i}{x_i} - \frac{y_j}{x_j} \right)^2 \right] \geq 0$$

B , therefore, is positive semidefinite with respect to the inner product given by Eq. A1 and its eigenvalues are nonnegative.

Appendix B: Graham's Law and the Derived Flux Expressions

By inspection of matrix B , we observe that the eigenrow corresponding to the zero eigenvalue, λ_1 , is equal to

$$y_1 = \left(\frac{1}{\alpha_1}, \frac{1}{\alpha_2}, \dots, \frac{1}{\alpha_n} \right)^T \quad (\text{B1})$$

The derived flux expressions, Eqs. 31 and 33, may be written

$$-c [D_e^{E-S} \text{ or } D_e^S] Z^{-1} A \nabla x = Z^{-1} N$$

For the first element of the above vector equation we have—using the fact that the rows of Z^{-1} are the eigenrows of B —that

$$-c [D_{1e}^{E-S} \text{ or } D_{1e}^S] y_1^T A \nabla x = y_1^T N \quad (\text{B2})$$

Using Eq. B1 and the definition of A , Eq. 30, we have that

$$y_1^T A \nabla x = \nabla \sum_{i=1}^n x_i = 0 \quad (\text{B3})$$

Introducing Eq. B3 in Eq. B2 gives

$$y_i^T \underline{N} = \sum_{i=1}^n \frac{N_i}{\alpha_i} = 0 \quad (\text{B4})$$

But $\alpha_i \propto \sqrt{M_i}$, proving that the EMT-SFA and SFA flux models satisfy Graham's law for isobaric diffusion.

It is readily concluded from the proof presented above that Graham's law will be satisfied by any flux expressions derived using the procedure discussed for the analysis of multicomponent diffusion, however the auxiliary conductances defined in Eq. 27 are averaged over the pore size and orientation distributions. Notice that since the eigenrow belonging to the zero eigenvalue is orthogonal to $A \nabla x$, the corresponding effective diffusion coefficient, D_{1e}^{E-S} or D_{1e}^S , does not appear in the flux expressions.

Literature Cited

- Amundson, N. R., *Mathematical Methods in Chemical Engineering*, Prentice-Hall, Englewood Cliffs, NJ (1966).
- Blick, A., J. C. Lont, and W. P. M. van Swaaij, "Gasification of Coal-Derived Chars in Synthesis Gas Mixtures under Intraparticle Mass-Transfer-Controlled Conditions," *Chem. Eng. Sci.*, **41**, 1895 (1986).
- de Boor, C., *A Practical Guide to Splines*, Springer, New York (1978).
- Burganos, V. N., Ph.D. Diss., Univ. Rochester, NY (1987).
- Burganos, V. N., and S. V. Sotirchos, "Diffusion in Pore Networks. Effective Medium Theory and Smooth Field Approximation," *AIChE J.*, **33**, 1678 (1987).
- Černá, M., J. Zahradník, and P. Schneider, "A Simplified Description of Multicomponent Diffusion in Porous Media. I: Diagonalization of the Matrix of Effective Diffusion Coefficients," *Coll. Czech. Chem. Commun.*, **43**, 1 (1978).
- Chen, O. T., and R. G. Rinker, "Modification of the Dusty-Gas Equation to Predict Mass Transfer in General Porous Media," *Chem. Eng. Sci.*, **34**, 51 (1979).
- Cunningham, R. E., and R. J. J. Williams, *Diffusion in Gases and Porous Media*, Plenum, New York (1980).
- Deriagin, B. V., and S. P. Bakanov, "Theory of the Flow of a Gas in a Porous Material in the Near-Knudsen Region," *Tech. Phys.*, **2**, 1904 (1957).
- Feng, C., and W. E. Stewart, "Practical Models for Isothermal Diffusion and Flow of Gases in Porous Solids," *AIChE J.*, **12**, 143 (1973).
- Gavalas, G. R., and S. Kim, "Periodic Capillary Models of Diffusion in Porous Solids," *Chem. Eng. Sci.*, **36**, 1111 (1981).
- Hirschfelder, J. O., C. F. Curtiss, and R. B. Bird, *Molecular Theory of Gases and Liquids*, Wiley, New York (1954).
- Jackson, R., *Transport in Porous Catalysts*, Elsevier, Amsterdam (1977).
- Johnson, M. F. L., and W. E. Stewart, "Pore Structure and Gaseous Diffusion in Solid Catalysts," *J. Catal.*, **4**, 248 (1965).
- Kirkpatrick, S., "Percolation and Conduction," *Rev. Mod. Phys.*, **45**, 574 (1973).
- Mason, E. A., and A. P. Malinauskas, *Gas Transport in Porous Media: The Dusty-Gas Model*, Elsevier, New York (1983).
- Mason, E. A., A. P. Malinauskas, and R. B. Evans III, "Flow and Diffusion of Gases in Porous Media," *J. Chem. Phys.*, **46**, 3199 (1967).
- Nicholson, D., and J. H. Petropoulos, "Capillary Models for Porous Media. VII: Study of Gaseous Flow in the Transition from the Knudsen to the Counter-Diffusion Regimes," *J. Phys. D: Appl. Phys.*, **10**, 2423 (1977).
- Satterfield, C. N., *Mass Transfer in Heterogeneous Catalysis*, MIT, Cambridge (1970).
- Scott, D. S., and F. A. L. Dullien, "Diffusion of Ideal Gases in Capillaries and Porous Solids," *AIChE J.*, **8**, 113 (1962).
- Silveston, P. L., "Multicomponent Diffusion in Capillaries," *AIChE J.*, **10**, 132 (1964).
- Sørensen, J. P., and W. E. Stewart, "Collocation Analysis of Multicomponent Diffusion and Reaction in Porous Catalysts," *Chem. Eng. Sci.*, **37**, 1103 (1982).
- Sotirchos, S. V., and N. R. Amundson, "Diffusion and Reaction in a Char Particle and in the Surrounding Gas Phase. A Continuous Model," *Ind. Eng. Chem. Fundam.*, **23**, 191 (1984).
- Stewart, W. E., and R. Prober, "Matrix Calculation of Multicomponent Mass Transfer in Isothermal Systems," *Ind. Eng. Chem. Fundam.*, **3**, 224 (1964).

Manuscript received Nov. 17, 1987, and revision received Jan. 26, 1988.